Time Sequence Change-Point Model of Electrostatic State Parameters of Aircraft Engine

Fu Yu[1*], *Wei Dongdong*[1], *Zuo Hongfu*[2], *Feng Zhengxing*[1]

1. College of Aeronautical Engineering, Civil Aviation University of China, Tianjin 300300, P. R. China;
2. College of Civil Aviation, Nanjing University of Aeronautics and Astronautics, Nanjing 210016, P. R. China

(Received 23 October 2017; revised 2 December 2017; accepted 16 January 2018)

Abstract: Electrostatic monitoring technology of particle charging information can facilitate online monitoring of aero-engine, which effectively enhances engine fault diagnosis and health managements. Unlike traditional engine state monitoring technologies, aircraft engine monitoring by gas path electrostatic monitoring not only covers the predicted information source itself, but also detects the information that can provide an early warnings for initial fault states through gas path charging levels. This paper establishes a non-stationary time sequence change-point model for anomaly recognition of electrostatic signals based on change-point theory combined with difference method of non-stationary time series. Finally, electrostatic induction data were utilized by the engine life test for a particular aircraft to validate the proposed algorithm. The results indicate that the activity level and the event rate were 0.5—0.8 (nc) and 50%, respectively, which were far greater than 4—12 (pc) and 0—4% under normal working conditions of the engine.

Key words: aero-engine; state identification; electrostatic monitoring technology; time series; change-point statistics

CLC number: Th165.3 **Document code**: A **Article ID**: 1005-1120(2018)01-0126-09

0 Introduction

Condition monitoring and fault diagnosis of aircraft engines are effective means to guaranteeing air safety and reduce maintenance costs. Engine monitoring system (EMS), prognostics and health management[1] (PHM) have been recently further developed toward condition monitoring technology to realize condition-based maintenance (CBM)[2]. Although traditional monitoring and diagnosis technologies hold advantages in aviation safety and economic efficiency, they are limited by the principle of monitoring means with many defects.

In bore-detection based on internal damage detection, the light source is limited by the endoscopic diameter. The internal structure of the engine is complex, and it presents an irregular geometric shape. Under the illumination of point light sources, many shadow areas will be easily generated in the image. These drawbacks hinder the extraction of image features and the subsequent diagnosis[3-4].

In vibration monitoring and diagnostic technology, abnormal vibration (i.e., vibration generated under normal engine operation) is accompanied by strong background signals, making abnormal signals difficult to capture accurately[5-6]. In addition, measured vibration signals can reflect only the overall vibration of engine, and the abnormal vibration is concealed in the macroscopic system-level vibration. Therefore, this technology is not ideal for fault localization.

In gas path performance parameter monitoring technology[7-8], the deficiency of this method lies in its poor reaction capability to short-term performance change of the engine[9]. Moreover,

* Corresponding author, E-mail address: fuyu00_@163.com.

How to cite this article: Fu Yu, Wei Dongdong, Zuo Hongfu, et al. Time sequence change-point model of electrostatic state parameters of aircraft engine[J]. Trans. Nanjing Univ. Aero. Astro., 2018,35(1):126-134.
http://dx.doi.org/10.16356/j.1005-1120.2018.01.0126

the system structure of the aircraft engine is extremely complex and the operating environment is harsh, leading to poor fault diagnosis capacity and localizing depth.

Gas-path electrostatic monitoring is an approach for intelligent health management of on-line monitoring early-stage faults. An increasing amount of literature on its methodologies, applications, and experiments has been presented in recent years. Vatazhin et al.[10] presented the theoretical method, laboratory modeling and simulation of electrostatic monitoring for engine. The electrostatic monitoring technology was also used in engine diagnostics through monitoring the overall electrostatic charge level. Considering the great potential of electrostatic monitoring, Fisher et al.[11] conducted an on-line monitoring experiment on gas path debris using electrostatic sensors. They reported that the electrostatic monitoring technology would be an important PHM tool. Powrie et al.[12] applied this technology to the PHM system of aero-engines. The inlet debris monitoring system and exhaust debris monitoring system (EDMS), using the electrostatic monitoring, were also developed and applied to a certain type of joint-fighter. Wilcox et al.[13] investigated the application in industrial gas turbines for gas path condition monitoring and discussed the sensor installation issues. Addabbo et al.[14-15] presented a theoretical modeling of an electrostatic gas path debris detection system and conducted an experimental validation. A similar research was conducted by the RMS Center of Nanjing University of Aeronautics and Astronautics in China. Wen et al.[16-17] optimized the electrostatic sensor design and conducted a simulated experimental study with a simulation test bench. Fu et al.[18-19] conducted a verified electrostatic monitoring experiment on a certain type of turbojet engine. Yin et al.[20] conducted a verified electrostatic monitoring experiment on a certain type of civil turbofan engine accordingly, and found a blade case rubbing fault and combustion fault.

Combining gas-path electrostatic with the change-point analysis method[21] of time sequence AR (P) model, we diagnosed the occurrence of a corresponding fault and further localized the damaged component and the damage degree. The proposed diagnosis method has the following advantages: Guaranteed air safety, reduced cost, and improved service efficiency of aircraft, and so on.

1 Formulation of Change-Point Model

The change-point model is defined as "one or a number of points that suddenly change in the model". This problem involves a sequence of samples in a chronological order. At an unknown time t, the mathematical features or statistical distribution of these samples suddenly change. Thus, t is called the change point at this time. For convenience, in the unary linear regression change-point model, we assume that : X is an independent variable, Y is a dependent variable, and n times of observed values are taken; i. e., (X_i, Y_i), $i=1,2,\cdots,n$. The model is set when $i=1,2,\cdots,m-1$, (X_i, Y_i) follows the linear regression model, that is

$$Y_i = a_1 + b_1 X_i + e_i \tag{1}$$

When $i=m, m+1, \cdots$; (X_i, Y_i) follows linear regression

$$Y_i = a_2 + b_2 X_i + e_i \tag{2}$$

where e_i is a random error in the model, a_1 and a_2 are the constant terms, b_1 and b_2 the independent variable coefficients of the equation, and Y_i is the i-th valuation of the dependent variable. At least one of $a_1 = a_2$ and $b_1 = b_2$ is false. At point m, if the coefficients of this regression equation are unequal, m is called the regressive change point.

2 Time Sequence Change-Point Model

2.1 Difference calculation

Most time series are non-stationary, and they could not accord with the precise demand to analyze aero-engine condition by change-point model of stationary time series. To realize a refined analysis of the aircraft engine state, stationary processing of the sample data must be conducted. At present, non-stationary time se-

quences are analyzed by using certain factor decomposition method, and difference method is a convenient and effective technique for information extraction. After the original data are stabilized with difference method, the stable time sequence change-point model (we take AR (P) as an example) can be used to analyze the identification of change points.

For any p-order auto-regression AR (P) process

$$x_t = \varphi_1 x_{t-1} + \varphi_2 x_{t-2} + \cdots + \varphi_p x_{t-p} + \varepsilon_t \quad (3)$$

where x_t is the observed value at time t; p the order of auto-regression; φ_1, $\cdots$, φ_p are the auto-regression coefficients; and ε_t is the white noise series.

The discrete-time sequence of p order difference is equal to p order derivation of the continuous time series. According to Cramer decomposition theorem, certain information in the sample sequence $\{x_t\}$ can be sufficiently extracted from the p order difference. Taking first-order difference as an example

$$X_t = \nabla X_t + X_{t-1} \quad (4)$$

This equation indicates that the essence of the first-order difference is an auto-regression process, that is, historical data $\{x_t\}$ after one-phase delay are used as independent variables to explain the change in date value $\{x_{t-1}\}$ in the current phase. Thus

$$\nabla^d X_t = (1-B)^d X_t = \sum_{i=0}^{d} (-1)^i C_d^i X_{t-i} \quad (5)$$

where B is the backward shift operator, $B^m X_t = X_{t-m}$, m the time span, ∇ the backward difference operator, $\nabla X_t = X_t - X_{t-1} = (1-B) X_t$, d the times of difference. The AR (P) model can be obtained through the deformation of Eq. (4). Under suitable difference order operation, certain formation contained in the data can be sufficiently extracted by applying Cramer decomposition theorem.

2.2 Model analysis

Random dynamic data in time sequence are arranged according to time order. According to before-after correlation of dynamic data, a convenient and feasible AR (P) (p-order auto regression model) model is used to establish the time sequence change-point model. Its descriptions are as follows: A sequence of observed values $\{x_t\}$, $t=1,2,\cdots,N$ meet the following auto regression model

$$x_t = \begin{cases} \varphi_1 x_{t-1} + \varphi_2 x_{t-2} + \cdots \varphi_p x_{t-p} + a_t \\ \qquad 1 \leqslant t \leqslant m \\ \varphi_1' x_{t-1} + \varphi_2' x_{t-2} + \cdots \varphi_{p'}' x_{t-p'} + a_t \\ \qquad m \leqslant t < N \end{cases} \quad (6)$$

If $\phi = (\varphi_1, \cdots, \varphi_p)^\tau \neq \phi' = (\varphi_1', \cdots, \varphi_p')^\tau$, Eq. (6)is called the discrete auto-regression time sequence change-point model, where m is the change point in the model, coefficients $\phi = (\varphi_1, \cdots, \varphi_p)^\tau$ and $\phi' = (\varphi_1', \cdots, \varphi_p')^\tau$ represent auto regression parameters, and residual error a_t is the white noise series.

2.3 Estimation and inspection of change points

(1) Roll investigated sample sequence

First, the sample length n and the investigation interval length n_0 are determined. That is, the sample data sequence is set as $\{X_t\}, t=1,2,\cdots,N$, the total data sequence length n is the length of the phase I sample, the interval $n_0 (n_0 \leqslant n \leqslant N)$ is rolled to divide the total data sequence into several subsequences: The first phase $\{x_1, x_2, \cdots, x_n\}$, the second phase $\{x_{n+1}, x_{n+2}, \cdots, x_{n+n}\}$, $\cdots$, the m-th phase $\{x_{(m-1)n+1}, x_{(m-1)n+2}, \cdots, x_{(m-1)n+n}\}$; the "rolling" analysis is conducted on the subsequences.

(2)Establish time sequence AR (k) model

① When $k=1,2,\cdots,m-1$, k<n, parameters $\varphi_{k1}, \varphi_{k2}, \cdots, \varphi_{kk}$ of AR (k) model are calculated as follows

$$\begin{cases} \bar{\omega}_{11} = \rho_1 \\ \bar{\omega}_{k+1,k+1} = \left(\rho_{k+1} - \sum_{j=1}^{k} \rho_{k+1-j} \bar{\omega}_{kj}\right) \left(1 - \sum_{j=1}^{k} \rho_j \bar{\omega}_{kj}\right)^{-1} \\ \bar{\omega}_{k+1,j} = \bar{\omega}_{kj} - \bar{\omega}_{k+1,k+1} \bar{\omega}_{k,k+1-j}; j = 1,2,\cdots k \end{cases} \quad (7)$$

In Eq. (7), p_j is the autocorrelation function and is estimated through the samples as follows

$$\rho_j = \frac{\gamma_j}{\gamma_0}$$

$$\gamma_j = \frac{1}{n} \sum_{t=j+1}^{n} (x_t - \bar{X})(x_{t-j} - \bar{X}) \quad (8)$$

② The residual sum of squares of the AR (k)model recurred: $k=1,2,\cdots,m$

$$S_k = S_0 \prod_{j=1}^{k} (1-\tilde{\omega}_{jj}^2) = (1-\tilde{\omega}_{kk}^2) S_{k-1}$$

$$S_0 = \sum_{t=1}^{n} (x_t - \overline{X})^2 \tag{9}$$

③ The amount of information BIC (k), $k=1,2,\cdots,m$ of the AR (k) model is calculated as follows

$$\mathrm{BIC}(k) = n\ln(S_k/n) + k\ln n \tag{10}$$

④ P is solved, and then

$$\mathrm{BIC}(P) = \min_{1\leqslant k\leqslant m} \mathrm{BIC}(k) \tag{11}$$

The solved model is named AR (P), and its parameters are $\varphi_{p1},\varphi_{p2},\cdots,\varphi_{pp}$.

(3)Test judgment

Difference test is conducted on neighboring models. If the orders are the same and the coefficients are approximate, then the difference is insignificant; otherwise, F statistical judgment will be used

$$F = \frac{A_0 - A_1}{s} \Big/ \frac{A_1}{n-r} \tag{12}$$

where A_0 and A_1 are the residual sums of squares corresponding to subsequences in two different phases (calculation is shown in Eq. (9)), s is the difference of numbers of subsequence parameters in two different phases, and r is the number of high-order model parameters.

The confidence level α is provided in advance. The F_α value, which satisfies $F_\alpha(P(F\geqslant F_\alpha)=\alpha)$, is searched through the F distribution table. When $F>F_\alpha$, the subsequences of the two phases will be significantly different.

We consider one single change point as an example. If the subsequences of two neighboring phases are significantly different, t_0 is the terminal point of the early-phase subsequence, and the moments in section $[t_0-n_0, t_0+n_0]$ are taken as alternate change-point moments. When an alternative change-point moment is taken as the boundary, the total data sequence is divided into two segments for modeling. The statistical quantity F will then be calculated, and then the place with the most significant before-after difference value will be taken as the change-point estimation.

3 Model Application and Discussions

3.1 Data source

The data were provided by a particular turbojet engine test. This experiment was used to detect electrostatic particles in engine exhaust. To avoid the destruction of engine structure, the electrostatic sensor was installed at the outer bracket of the engine tailpipe. This test bench was applicable to all life tests for turbojets, and mainly used for overall performance, applicability performance, long performance and lifespan, etc. The test bench consisted of a thrust test bench system, a fuel oil supply system, and an electric control system. This experimental engine started a 200 h lifespan performance test in July 2011, and a 40 h test was added later, resulting in a total 240 h test). The interval of the test was 1 h. Electrostatic monitoring started from the 100th phase of life test and ended in the 240th phase. The first hour was removed because collection line was connected at the ground and it effectively monitored 139 phases. These data were collected on November 12, 2011 between 08:00 a. m.—10:00 a. m., and the searching interval was 1 min. The sampling site was as shown in Fig. 1.

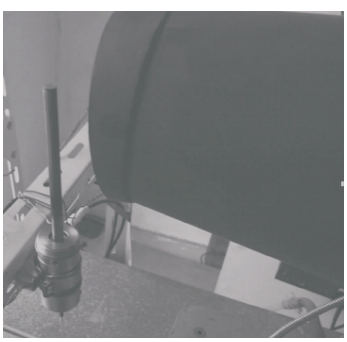

Fig. 1 Schematic of actual sampling site

(1)Background signals

According to Refs. [11-12], there are two important feature parameters in engine electro-

static signal analysis, namely, activity level and event rate, which are calculated as follows:

①Activity level (AL): The activity level reflects the quantity of small particles (such as soot particles and fraction-lets) that continuously appear within a period of time T, and it is a measurement of ratio-frequency components of signals. Activity level is defined as follows

$$AL = \sqrt{\frac{1}{N}\sum_{n=1}^{N} Q_n^2} \tag{13}$$

where N is the number of samples within time T, and its activity level is the root-mean-square value.

② Event rate (ER): The event rate is used to measure the number of abnormal particles in airflow within unit time. Typical events include abnormal large particles generated by component fault and large soot particles generated by incomplete combustion. Event rate is expressed as follows

$$\mathrm{ER}(t) = \frac{M}{N} \cdot 100\% \tag{14}$$

where M is the number of events within the time T, N the total number of samples within time T. The physical significance represented by the event rate is within a certain time interval (1 s) of the electrostatic sensor. The percentage of the number of points exceeding K times of charge of current interval AL value in the total number of sampled points.

In ignition phase after the experiment starts, a large quantity of positive and negative ions were generated inside the pipeline, resulting in a drastic change in the induced voltage on the sensor, as shown in Fig. 2(a), where A represents the amplitude of original data. After approximately 5 s, the combustion tends to stabilize, and so does the induced voltage on the sensor.

In Fig. 2(b), when the engine starts in the ignition phase, large soot particles generated by incomplete combustion are contained in tail gas, resulting in a major change in the activity level in the first 5 s. When the AL charge reaches 30 pc,

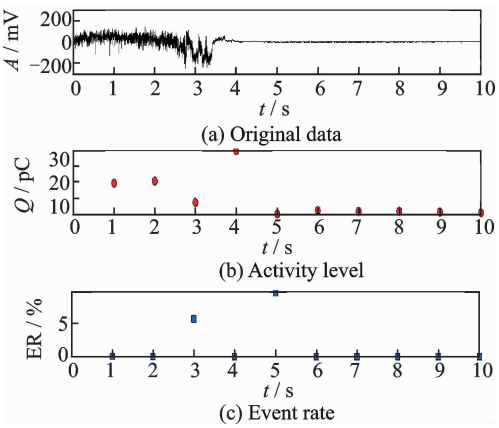

Fig. 2 Signal and its feature parameters in startup phase

the signal event rate ER in Fig. 2(c) ascends accordingly, and the largest proportion reaches 10%. When the engine is under normal operating status (after 5 s), combustion generates soot particles with minimal size (nanometer level). These soot particles are the main components of garpath charged particles. Moreover, the combustion process in the combustion chamber of the engine under normal operation is very stable. Thus, the generated soot particles are relatively stable, and the corresponding activity level and event rate tend to be 0. In the analysis chart in this paper, the activity level parameters are uniformly expressed by red solid dots "·", and event rates are expressed by blue solid square dots "■".

(3)Abnormal signal

This paper uses typical data monitored from 8:00 to 10:00 AM on November 12, 2011. The value on each sampled point represents the electrostatic signal of the tail gas that passes through the sensor in last 1 min. The data after difference stationary processes are taken as an example to establish the time sequence AR (P) change-point model

$$Q_t = \begin{cases} \varphi_1 Q_{t-1} + \varphi_2 Q_{t-2} + \cdots \varphi_p Q_{t-p} + a_t \\ 1 \leqslant t \leqslant m \\ \varphi_1' Q_{t-1} + \varphi_2' Q_{t-2} + \cdots \varphi_{p'}' Q_{t-p'} + a_t \\ m \leqslant t < N \end{cases} \tag{15}$$

where Q is the tail-gas electrostatic induction signal detected by the sensor, where m is the change point in the model, coefficients $\phi = (\varphi_1, \cdots, \varphi_p)^\tau$, $\phi' = (\varphi_1', \cdots, \varphi_p')^\tau$ represent auto-regression pa-

rameters, and the residual error a_t is the white noise series. The model significance is shown in Eq. (6). Fig. 3 shows the original data curves of the electrostatic signals.

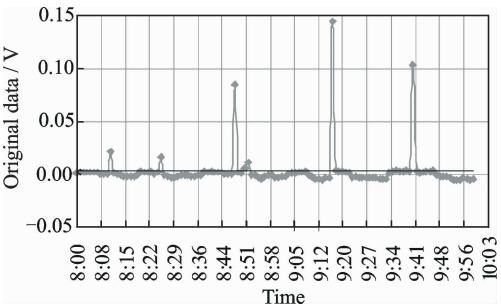

Fig. 3 Original data curves acquired by sensor

3.2 Stabilizations method

After the first-order difference of the original time sequence data (Fig. 3) $\{Q_t\}$ of sensor in Fig. 1 recorded as $\{\nabla Q_t\}$, $\nabla Q_t = Q_t - Q_{t-1}$, $\{\nabla Q_t\}$ is as shown in Fig. 4.

As shown in Figs. 3, 4, the original sequence Q_t has linear ascending and descending tendencies, and sequence $\{\nabla Q_t\}$ after difference has been stablizied nearby a fixed value.

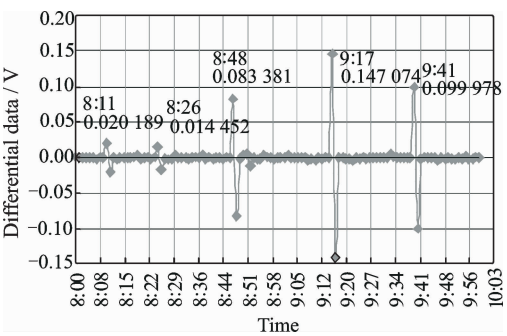

Fig. 4 Original data first-order difference

3.3 Change-point searching algorithm flow

The change-point searching algorithm in Section 3 can rapidly and accurately detect the time position at which quantitative change of electrostatic data occurs. The specific searching steps are as shown in Fig. 5.

3.4 Test results

The test level is set as $\alpha=0.05$. The parameters are calculated according to Eqs. (7—12) and then used to test the existence of the change points. The calculation results are shown in Table 1.

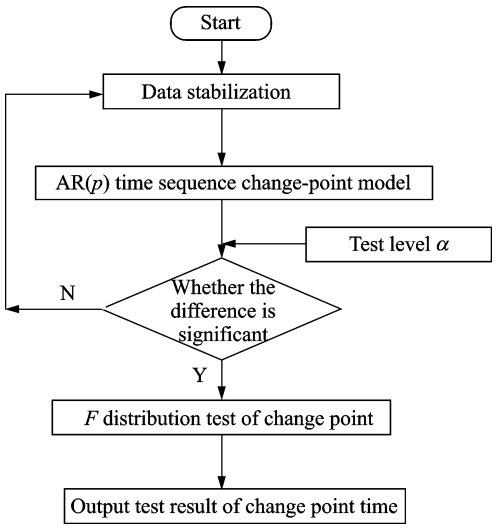

Fig. 5 Change-point searching flowchart

Table 1 Change-point searching results

Start	End	Jumping degree	$\alpha=0.05y/n$	Change-point time
8:00	8:01	−0.000 13	n	n
8:01	8:02	0.000 668	n	n
8:02	8:03	−0.000 02	n	n
⋮	⋮	⋮	⋮	⋮
8:10	8:11	0.020 189	y	8:11
8:11	8:12	−0.019 99	y	8:11
8:12	8:13	−0.000 23	n	n
⋮	⋮	⋮	⋮	⋮
8:25	8:26	0.014 452	y	8:26
8:26	8:27	−0.016 99	y	8:26
8:27	8:28	−0.000 55	n	n
⋮	⋮	⋮	⋮	⋮
8:47	8:48	0.083 381	y	8:48
8:48	8:49	−0.082 21	y	8:48
8:49	8:50	−0.000 95	n	n
⋮	⋮	⋮	⋮	⋮
9:16	9:17	0.147 074	y	9:17
9:17	9:18	−0.140 25	y	9:17
9:18	9:19	−0.000 29	n	n
⋮	⋮	⋮	⋮	⋮
9:40	9:41	0.099 978	y	9:41
9:41	9:42	−0.100 15	y	9:41
9:42	9:43	−0.001 08	n	n
⋮	⋮	⋮	⋮	⋮

Change-point searching results show that change points appear five times at 8:11 a. m., 8:26 a. m., 8:48 a. m., 9:17 a. m., and 9:41

a. m. Meanwhile, the engine produces a loud, abnormal sound. Detection by test personnel after disassembly revealed that large-particle carbon deposits appear in the combustion chamber (Fig. 6). The real-world scenario verifies that this paper can perform real-time monitoring of change status of gas-path charging level of the engine to provide early warning of the initial fault status. Fig. 7 shows the data and signal features acquired at a typical change-point time 08:11 a. m.

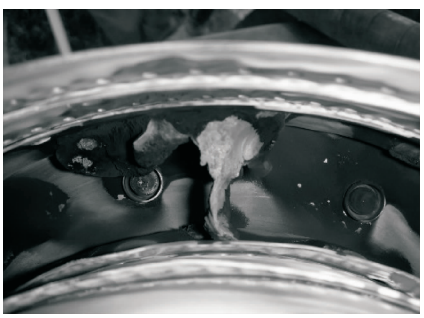

Fig. 6 Carbon deposit in fuel spray nozzle

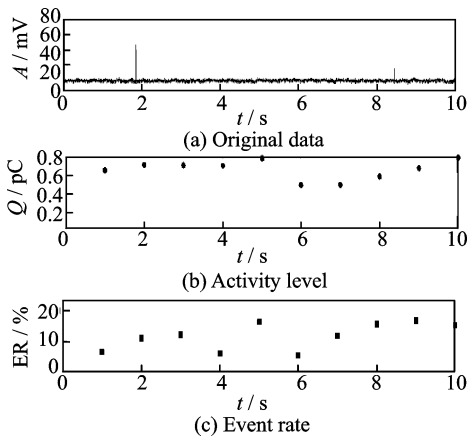

Fig. 7 Electrostatic signals and features at typical change-point time

Comparisons of Figs. 2(b, c) and Figs. 7(b, c) show that the activity level and event rate after the engine starts and stabilizes tend to be 0. However, when the change point occurs, a corresponding activity level AL is maintained at a stable level 0.5—0.8 (nc), and the proportion of the corresponding event rate reaches 50%, which is far greater than the stable status under normal operation of the engine. Actual operation of the engine shows that normal background noise signals are at milli-volt levels, but obvious abnormal pulse amplitude appears within the period of the 216th—217th test run and even volt-level signals appear.

4 Conclusions

The time sequence change-point model established in this paper rapidly and effectively detects the time when quantitative change occurs.

(1) Within 5 s in the engine ignition phase, the induced voltage amplitude experiences obvious change; the corresponding activity level is 30 pc and event rate is approximately 10%. After it stabilizes, both the activity level and event rate of the induced signals return to a value near 0.

(2) The activity level at a typical change-point time is maintained at 0.5—0.8 (nc) and the event rate reaches 50%, both of which are far greater than the level under stable working conditions.

(3) Based on the above searching algorithm, results show that five change-point times, namely, 8:11 a. m., 8:26 a. m., 8:48 a. m., 9:17 a. m., and 9:41 a. m., are detected, and the corresponding jumping degrees are 0.020 189, 0.014 452, 0.083 381, 0.147 074, and 0.099 978. Normal background noise signals of the engine are at millivolt level, but volt-level signals appear at change-point time. This finding indicates that excess soot particles are present at change-point time, and these abnormalities change the charging level of the charged particles in the gas path. The engine disassembly report shows that large-particle carbon deposits can be found in the combustion chamber, and change-point results of electrostatic induction signals determine the corresponding fault reflection.

(4) Difference method can concisely and effectively extract certain information. After the original data are processed by the first-order differential formula, linear trend terms of this data sequence are effectively eliminated, thereby facilitating the extraction of information while the sample sequence is smoothed.

(5) As an advanced early fault detection

method, the change-point model can reflect the working conditions of the engine. This model is beneficial to improving monitoring techniques and realizing fault prediction and health management.

Acknowledgements

The work is supported by the Initial Scientific Research Fund (No. 2015QD02S), the Foundation Research Funds for the Central Universities (No. 3122016A004, 3122017027), which are highly appreciated by the authors.

References:

[1] GUO Y M, CAI X B, ZHANG B Z. Review of prognostics and health management technology [J]. Computer Measurement & Control, 2008, 16(9): 1213-1216.

[2] ROEMER M J, KACPRZYNSKI G J, SCHOELLER M H. Improved diagnostic and prognostic assessments using health management information fusion [C]// 2001 IEEE Systems Readiness Technology Conference. Valley Forge, PA: IEEE, 2001: 365-377.

[3] YU H, ZUO H F, HUANG C Q. Advanced endoscopy and fault testing of aeronautic engine [J]. Aviation Engineerging & Mainienance, 2002(2): 20-22.

[4] LI C Y, SHI H, YAO H Y. Research on borescope image properties[J]. Testing Equipment & Trchnology, 2006, 239(5): 38-40.

[5] CHEN G, LI C G, WANG D Y. Nonlinear dynamic analysis and experiment verification of rubbing faults of rotor-ball bearing-support-stator coupling system for aero-engine [J]. Journal of Aerospace Power, 2008, 23(7): 1304-1311.

[6] CHEN G. Vibration modeling and analysis for dual-rotor aero-engine [J]. Journal of Vibration Engineering, 2011, 24(6): 619-632.

[7] VODOPIANOV V, NIKITIN V. A new approach to GPA-system for gas turbine engine [C]// The 39th AIAA/ASME/SAE/ASEE Joint Propulsion Conference and Exhibit. Huntsville, Alabama: AIAA, 2003: 4986.

[8] ROMESSIS C, MATHIOUDAKIS K. Bayesian network approach for gas path fault diagnosis [J]. Journal of Engineering for Gas Turbines and Power, 2006, 128(1): 64-72.

[9] LI Y G. A gas turbine diagnostic approach with transient measurements [J]. Proceedings of the Institution of Mechanical Engineers, Part A: Journal of Power and Energy, 2003, 217(2): 169-177.

[10] VATAZHIN A, STARIK A, KHOLSHCHEVNIKOVA E. Electric charging of soot particles in aircraft engine exhaust plumes[J]. Fluid Dynamics, 2004, 39(3): 384-392.

[11] FISHER C. Data and information fusion for gas path debris monitoring [C]// Aerospace Conference, 2001, IEEE Proceedings. [S. l.]: IEEE, 2001: 3017-3022.

[12] POWRIE H, NOVIS A. Gas path debris monitoring for F－35 Joint Strike Fighter propulsion system PHM[C]// Aerospace Conference. [S. l.]: IEEE, 2006: 8.

[13] WILCOX M, RANSOM D, HENRY M, et al. Engine distress detection in gas turbines with electrostatic sensors[C]// ASME Turbo Expo 2010: Power for Land, Sea, and Air. Marine Glasgow, UK: [s. n.], 2010: 39-51.

[14] ADDABBO T, FORT A, MUGNAINI M, et al. Theoretical modeling of an electrostatic gas-path debris detection system with experimental validation [C]// Proceedings of 2015 IEEE Sensors Applications Symposium. Zadar, Croatia: [s. n.], 2015: 13-15.

[15] ADDABBO T, FORT A, GARGIN R, et al. Theoretical characterization of a gas path debris detection monitoring system based on electrostatic sensors and charge amplifiers [J]. Measurement, 2015, 64: 138-146.

[16] WEN Z H, ZUO H F, LI Y H. Gas path debris electrostatic monitoring technology and experiment [J]. Journal of Aerospace Power, 2008, 23(12): 2321-2326.

[17] WEN Z, MA X, ZUO H F. Characteristics analysis and experiment verification of electrostatic sensor for aero-engine exhaust gas monitoring [J]. Measurement, 2014, 47(1): 633-644.

[18] FU Y, ZUO H F, LIU P P, et al. Gas path electrostatic sensors monitoring and comparison experiment on turbojet engine [J]. Transactions of Nanjing University of Aeronautics & Astronautics, 2013, 30(4): 361-365.

[19] FU Y, YIN Y B, WANG H, et al. Study on detection for aero-engine abnormal condition based on permutation entropy of electrostatic signal [J]. Automation & Instrumentation, 2017(11): 1-5, 19.

[20] YIN Y, CAI J, ZUO H, et al. Experimental investigation on electrostatic monitoring technology for civil turbofan engine [J]. Journal of Vibroengineering, 2017, 19(2): 967-987.

[21] FU Y. Recognition for change-point of traffic flow binary linear regressions based on projective transform method [J]. Journal of Computer Applications,

2010, 30(1):263-262.

Dr. **Fu Yu** is currently a lecturer in College of Aeronautical Engineering, Civil Aviation University of China. He received the Ph. D. degree in Traffic Information Engineering and Control from Nanjing University of Aeronautics and Astronautics, China, in 2014. He has a wide interest in gas path monitoring for aero-engine including data analysis, signal processing and fault diagnosis.

Mr. **Wei Dongdong** received the B. Sc. in School of Mechatronics Engineering from Zhengzhou University of Aeronautics, Zhengzhou, China, in 2015. He is currently a postgraduate student at the Aeronautical Engineering Institute, Civil Aviation University of China. His research is focused on aero engine maintenance.

Prof. **Zuo Hongfu** received B. Sc. degree and Ph. D. degrees both from China University of Mining and Technology in 1985 and 1989, respectively. Now, he is a professor and doctoral supervisor in Nanjing University of Aeronautics and Astronautics. His main research field covers system testability, fault prognosis, reliability engineering, state monitoring and fault diagnosis of aircraft engine, maintenance decision and optimization.

Mr. **Feng Zhengxing** received the M. Sc. degree in Superior Institute of Aeronautic and Aerospace (ISAE, France). He is currently an assistant lecturer at the Aeronautical Engineering Institute, Civil Aviation University of China. His research is focused on aero engine thermodynamic analysis.

(Production Editor: Zhang Bei)